Figure 2. Seasonal sea-surface salinity distribution. **(a)** Winter (November – March) and **(b)** summer (June – September) (Sofianos et al., 2003). Seasonal sea-surface temperature distribution and averaged net surface currents. **(c)** Winter (October – April) and **(d)** summer (May – September) (Raitos et al., 2013, 2015).
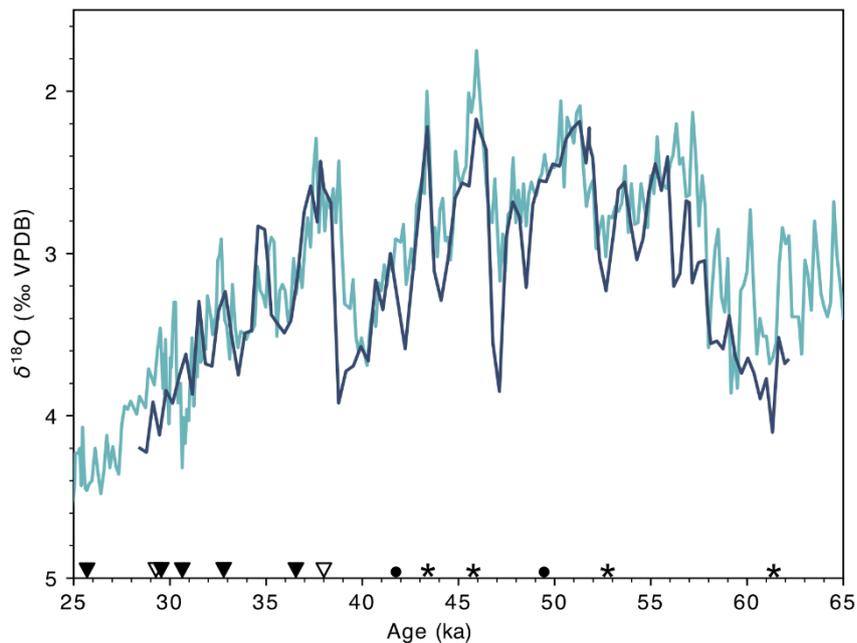

Figure 4. Alignment of benthic $\delta^{18}O$ records of cores KL11 from the central Red Sea (dark blue) and GeoB5844-2 from the northern Red Sea (light blue). Black triangles represent the radiocarbon dates, and black dots the paleomagnetic data used for the establishment of the age model of GeoB5844-2 (Arz et al., 2007). The

age model of KL11 is based on two radiocarbon dates of KL11 (white triangles; Schmelzer, 1998) and the graphical correlation of the δ¹⁸O records. Black asterisks represent the graphical tie-points.
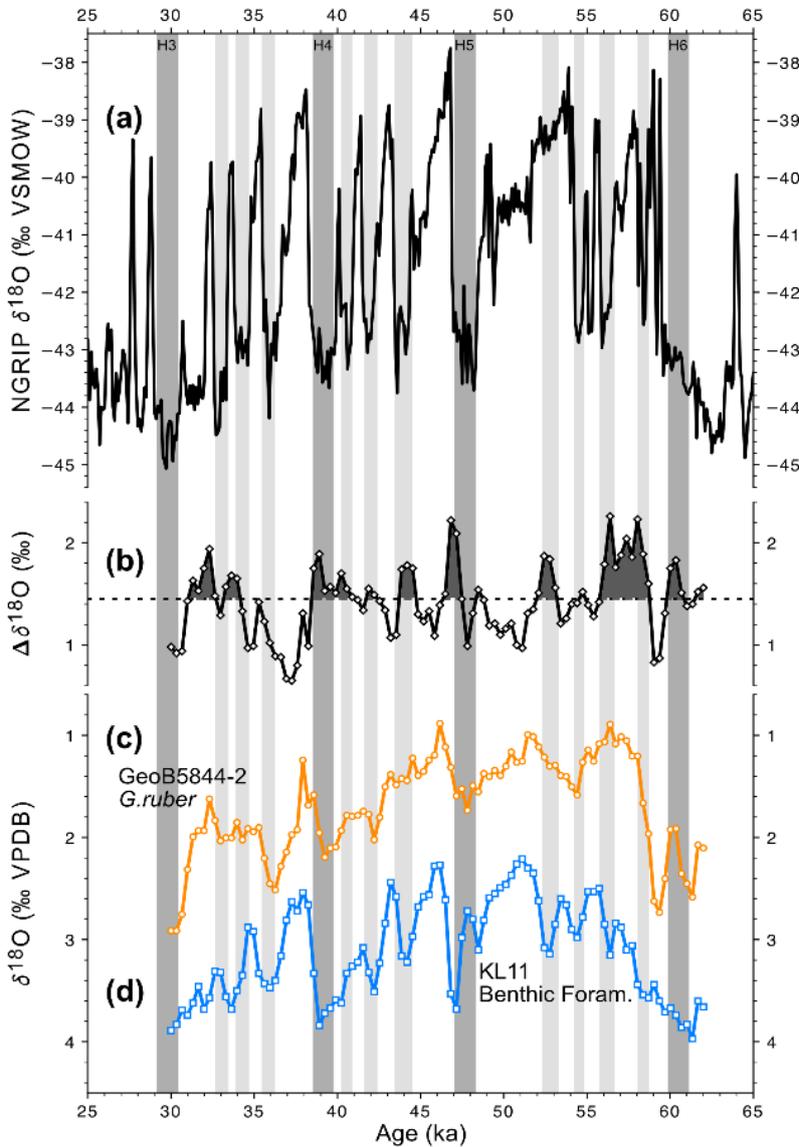

Figure 7. Comparison of epibenthic and planktic stable oxygen isotope records from the Red Sea, their resulting difference, and the Greenland stable oxygen isotope record. **(a)** $\delta^{18}O$ record of the North Greenland Ice Core Project (NGRIP members, 2004) against the extended GICC05 age scale (Svensson et al., 2008; Wolf et al., 2010). **(b)** Difference in the stable oxygen isotope records ($\Delta\delta^{18}O$) of **(d)** the composite epibenthic $\delta^{18}O$ of KL11 from the central Red Sea and **(c)** the planktic (*Globigerinoides ruber*) $\delta^{18}O$ of GeoB5844-2 from the northern Red Sea (Arz et al., 2007). For calculation of the $\Delta\delta^{18}O$ values, the single records were resampled at a spacing of 330 years. The stippled line in the $\Delta\delta^{18}O$ record marks the mean value. Grey bars represent northern hemisphere stadials and Heinrich events.